Proceedings of the Institute of Acoustics

BLIND SEPARATION OF SIGNAL AND MULTIPATH INTERFERENCE FOR SYNTHETIC APERTURE SONAR

I.P. Kirsteins Naval Undersea Warfare Center, 1176 Howell St, Newport, RI 02841 USA

1 BACKGROUND

High resolution acoustic images of the sea floor are needed in applications such as mapping, mine hunting, cable and pipeline surveying, and underwater archaeology. One important imaging technique is synthetic aperture sonar (SAS). Fine cross-range resolution is obtained by using the motion of the sonar platform to synthesize a much larger virtual acoustic aperture or baseline than the sonar's physical aperture by coherently combining multiple pings. However, SAS imaging becomes problematic at long ranges because of multipath interference (see fig. 1). The multipath interference results in additive snow-like noise corruption of the SAS image due to the ping-to-ping decorrelation of surface bounce paths by sea surface roughness, filling in object shadows.

Multipath interference can be suppressed using a receiver with vertical directivity since the direct and surface bounce paths have different arrival angles. However, in most realistic scenarios an impractically large vertical aperture will likely be needed at long ranges (path angles become close as range increases) to obtain adequate multipath rejection if using conventional delay-sum beamforming (steering a beam toward the bottom). Acceptable multipath rejection with a small array is only attainable using either adaptive interference cancellation or null steering.

The objectives of this paper are (1) to experimentally demonstrate with actual in-water SAS data the blind separation of the direct path signal from the surface bounce multipath interference using a blind algorithm proposed in [2] that exploits differences in the ping-to-ping temporal coherence of the paths and (2) discuss the challenges and lessons learned from real data implementation. The motivation for using blind separation rather than conventional matrix inverse-based adaptive interference cancellation schemes such as Generalized Sidelobe Cancellers (GSCs) [1] is because blind methods do not need accurate array calibration and signal steering vector information, hence simplifying implementation, and furthermore, signal-free training data is not needed (signal and multipath interference are simultaneously present here).

The paper begins by reviewing the mathematical models for the signal and interference followed by optimum signal estimation and the blind separation algorithm. An initial version of the blind algorithm is implemented as a GSC-like hybrid algorithm (using signal and signal block beams calculated from the nominal test geometry, but still separated blindly) to maintain a constant signal response and tested on real SAS multipath data. The initial implementation reveals poor and unstable control of the signal response that resulted in artifacts in the constructed SAS image. Motivated by the challenge of maintaining a constant signal response in a blind algorithm, a modified version of the algorithm is developed that combines the GSC-like implementation with a blindly estimated signal blocking matrix and is shown to work well.

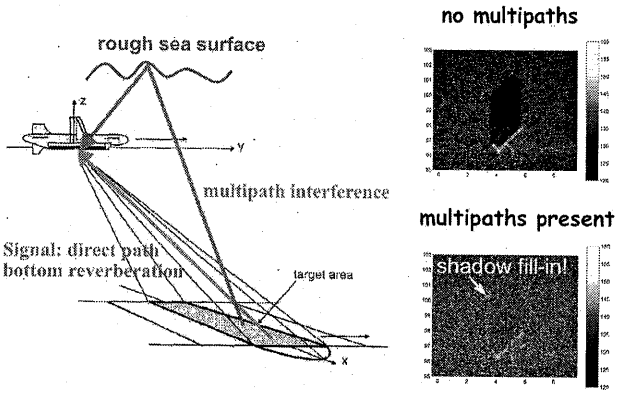

Figure 1. Multipath interference from surface bounce paths and simulated SAS images showing the effects of multipath interference. Observe that the multipath interference corrupts the image with snow-like noise and fills the objects acoustic shadow.

2 MATHEMATICAL MODEL OF SIGNAL AND INTERFERENCE

Assume that the SAS system has a planar receiving array and a point source transmitter. For the sake of brevity, the planar array is modeled as consisting of only two columns of equi-spaced hydrophones and a transmitter located at the center (see fig. 2a). Denote the complex vertical aperture sensor or beam output (at a given frequency) M×1 vectors containing the backscattered bottom signal and multipath components impinging on the leftmost and rightmost staves from some range cell in the kth ping cycle as $\vec{x}_k$ and $\vec{y}_k$ respectively. Mathematically, the frequency domain vector outputs from each respective stave are

$$\vec{x}_k = \underbrace{\alpha_k^x \vec{s}}_{\text{signal}} + \underbrace{\sum_{j=1}^{P} c_{jk}^x \vec{h}_j}_{\text{multipaths}} + \vec{n}_k^x \tag{1}$$

and

$$\vec{y}_k = \underbrace{\alpha_k^y \vec{s}}_{\text{signal}} + \underbrace{\sum_{j=1}^{P} c_{jk}^y \vec{h}_j}_{\text{multipaths}} + \vec{n}_k^y \tag{2}$$

where the vector $\vec{s}$ is the signal basis vector or array manifold, $\vec{h}_j$ is the basis vector of the jth multipath interference component, P is the number of interfering multipaths, α_k^x, α_k^y are the complex signal amplitudes, the c_{jk} are complex random variables corresponding to the interference amplitudes, and the elements of the background noise vector $\vec{n}_k^x, \vec{n}_k^y$ correspond to volume and surface reverberation and ambient noise.

A. Ping-to-Ping Coherence of Direct Path Signal

Ping-to-ping coherent bottom reverberation measurements are easily obtained from a SAS system. Each transmitter-receiver pair in fig. 2a constitutes a bistatic geometry. It has been shown that when the range to some local annulus of scatterers is essentially in the far-field (relative to the sensor pair basline), the bistatic receiver-transmitter pairs in the array can be approximated by equivalent fictitious monostatic receivers-transmitters located at their mid-points [3] (see fig. 2a). In other words, the backscattered signal time series measured from the seafloor (ignoring multipaths) by the bistatic receiver-transmitter pair is approximately as that measured by a single receiver-transmitter located at their phase center. If the speed of the SAS vehicle and the ping repetition rate are adjusted such that the array is displaced by distance d/2 between successive pings, the array phase centers overlap, as depicted in fig. 2b and each pair will measure the same reverberation. Thus for any pair of overlapping fictitious staves at pings k and k+1, we have $\alpha_k^x \approx \alpha_{k+1}^y$ and because of sea surface roughness, the multipaths are uncorrelated ping-to-ping, i.e. $E[c_{jk} c_{jk+1}^*] \approx 0$.

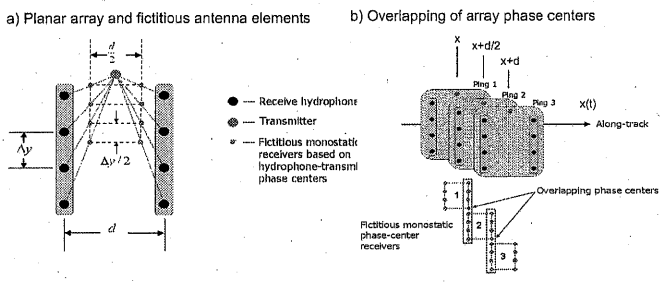

Figure 2. (a) Planar receiving array geometry and creation of fictitious monstatic elements using the phase centers of the receiver-transmitter pairs. (b) Overlapping vertical phase centers obtained by adjusting the ping repetition rate and the SAS vehicles forward speed.

3 BLIND SEPARATION

A. Optimum Estimation

The objective is to estimate the signal α_k^x from the noisy measurement $\vec{x}_k$. If the covariance matrix R of the interference were known, the best linear minimum mean-square error (MSE) estimator (also maximum signal-to-noise ratio) would be [1]

$$\hat{\alpha}_k = \vec{w}_{opt}{}^H \vec{x}_k \tag{3}$$

where the optimum filter weights are given by

$$\vec{w}_{opt} = R^{-1}\vec{s} / \vec{s}^H R^{-1}\vec{s} \tag{4}$$

Unfortunately, in this and most applications the interference covariance matrix R is not known beforehand. Also the signal steering vector $\vec{s}$ itself may not be known accurately.

B. Blind Separation Using Ping-to-Ping Coherence

We now describe and motivate the blind multipath separation algorithm proposed in [2]. Intuitively, since the signal is highly correlated or coherent ping-to-ping, $\alpha_k^x \approx \alpha_{k+1}^y$, and the multipaths are uncorrelated, $E[c_{jk} c_{jk+1}^*] \approx 0$, the filter weights for multipath suppression in principle could be

estimated by minimizing the phase differences between successive pings. Fig. 3a shows histograms of phase difference measurements obtained from actual experimental data for the multipath interference and direct path signal. We see that the direct path signal phase fluctuations are highly concentrated whereas the multipath phase differences are almost uniformly distributed as expected. Therefore, we propose estimating the weights by minimizing $\angle\vec{w}^H\vec{x}_n - \angle\vec{w}^H\vec{y}_{n+1}$ over n=1,2,...N. This approach does not need signal-free training data nor any prior signal steering vector or array calibration information and hence is *blind*, and furthermore, since it only depends on the ping-to-ping phase difference, it is invariant to fluctuations in the signal magnitude from transmitter instability and range differences. Direct numerical evaluation of the phase differences is problematic because their cyclical nature (modulo 2π) may require phase unwrapping. This difficulty is overcome by using the *circular variance* [4]. The *circular variance* (CV) is defined for given a set of angle measurements $\theta_1,\ldots,\theta_N$ as

$$cv[\theta_1,\ldots,\theta_N] = 1-\sqrt{\bar{x}^2+\bar{y}^2}$$
$$\bar{x} = 1/N\sum_{k=1}^{N}\cos\theta_k \;,\; \bar{y} = 1/N\sum_{k=1}^{N}\sin\theta_k \qquad (5)$$

and lies in the interval [0,1], with one corresponding to maximum variance. It is easy to evaluate numerically and used widely by the statistics community to analyze the dispersion of angular data such as wind and ocean current direction, fracture orientations, and animal movements. We therefore advocate estimating the filter weights by iteratively solving

$$\min\vec{w} \quad cv[\Delta\theta_1,\Delta\theta_2,\ldots,\Delta\theta_N] \qquad (6)$$

(see [2] for details) where $\Delta\theta_k = \angle\vec{w}^H\vec{x}_k - \angle\vec{w}^H\vec{y}_{k+1}$.

In regards to optimality, the CV is related to the maximum likelihood (ML) estimate of the concentration parameter of the von Mises distribution [4]. The von Mises distribution is often used to model circular or angular data and is considered to be the circular analog of the regular Gaussian distribution [4]. Additionally, the statistic $N(1\text{-}CV)^2$ corresponds to the Rayleigh test for testing phase uniformity [4]. This suggests that the CV should be a good measure of phase dispersion or coherence. In [2] it was shown that the blind separation algorithm is competitive with parametric high resolution methods and compared favorably to the Cramer-Rao lower bounds.

4 REAL IN-WATER SAS DATA DEMONSTRATION

A. Scenario

The blind separation algorithm is now demonstrated on actual shallow water SAS multipath interference data. A bottom-mounted rail SAS test system was used rather than a SAS vehicle for the data collection. The SAS receiver and transmitter assembly are similar to that shown in fig 2a. The ping-to-ping motion of the rail was adjusted to obtain overlapping antenna phase centers (as in fig. 2b) and the transmitted signal was a short sinusoidal pulse. Figure 3 shows ping-to-ping phase histograms and vertical delay-sum beamforming analysis of the data using thirty consecutive pings. We see that the multipath interference from the first single-bounce path is strong compared to the direct path signal, with considerable sidelobe leakage into the bottom beams at longer ranges (fig. 3b). Also, as expected, the multipath interference is approximately uncorrelated ping-to-ping whereas the direct path signal is highly correlated (fig. 3b).

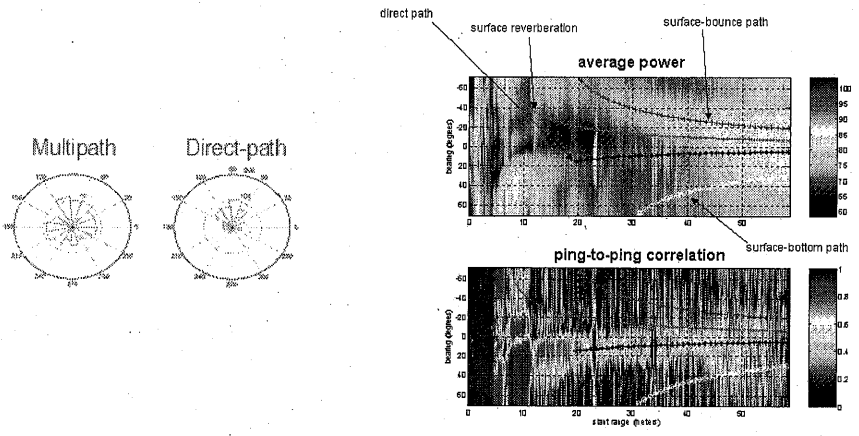

(3a) (3b)

Figure 3. (a) Histogram of ping-to-ping phase differences. (b) Vertical delay-sum beamforming analysis of thirty sequential pings as a function of vertical arrival angle and slant range. The upper plot shows the average power and the lower plot is the measured ping-to-ping correlation. Positive vertical angles correspond to directions toward the bottom whereas as negative angles correspond to the surface.

B. Initial Hybrid GSC-like Blind Algorithm Implementation

In order to reconstruct the time series from the spatially filtered frequency domain data, the estimated weight vector $\vec{w}'$ must be scaled such that a constant signal response is maintained, $\vec{w}'^{H}\vec{s} = c$, where c is some constant. However, the scaling factor c cannot be determined blindly and thus some ancillary information about the array or signal must be used for scaling. This is a problem inherent with blind source separation methods [5]. In real SAS systems there is prior array calibration and bottom pointing information available. We now assume that a reasonably accurate steering vector can be formed, although not perfect. Assuming a rough steering vector is available, the blind method in implemented as a GSC (see fig. 4) in order to maintain an approximately constant signal gain for time series reconstruction. Since the blind separation algorithm doesn't care about the data coordinate system, the GSC-like implementation should still be robust against array calibration and beam pointing errors.

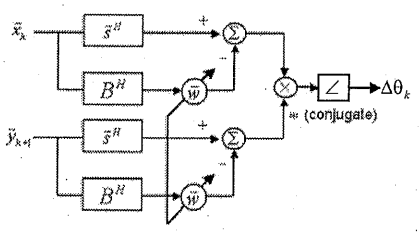

Fig. 4. GSC-like implementation of blind algorithm where $\vec{s}$ is the signal steering vector and B is the signal blocking matrix.

C. Experimental Results

A total of 120 pings were collected for SAS processing. Frequency domain data snapshots of the form in (1) were constructed by subdividing the time series of each channel into short intervals or range gates (length chosen so that the bottom signal and multipaths were approximately

stationary), FFTs computed for each interval, and the frequency bins then arranged into data vectors. The data set of 120 pings was broken up into subsets of 30 sequential pings and processed individually. The blind filter weights were estimated in each range gate using the GSC-like implementation of fig. 4 and the data vector then spatially filtered, with the blind estimate of the signal in the mth DFT bin given by

$$\hat{\alpha}_{bk}^{x} = \vec{w}_{blind}'^{H}(m)\,\vec{x}_k'(m) \tag{7}$$

with $\vec{x}_k'(m) = [\vec{s}_m^{\,H} \mid B]^H \vec{x}_k(m)$. For reference, the signal was also estimated via conventional beamforming, i.e. $\hat{\alpha}_{ck}^{x} = \vec{s}_m^{\,H}\,\vec{x}_k(m)$. The signal steering vector was calculated using the nominal experimental geometry.

The performance was evaluated by measuring the output ping-to-ping phase difference circular standard deviation [4] and the power and then plotting it as a function of slant range and frequency. Fig. 5a shows that the blind method has significantly reduced ping-to-ping phase dispersion when compared against the conventional beamformer, suggesting that the blind method is working well in suppressing the multipath interference. However, the blind method has large fluctuations in the output power (see fig. 5b), indicating that a constant signal response is not being maintained. This is not desirable because the gain fluctuations will introduce errors and artifacts into the SAS image.

If we examine the blind signal estimate

$$\hat{\alpha} = \vec{s}^{\,H}\vec{x} - \vec{w}_{blind}^{H} B^H \vec{x} \quad , \tag{8}$$

the likely culprit causing the large gain fluctuations is signal leakage by an erroneous signal blocking matrix (array calibration and signal beam pointing errors). Maintaining constant gain is a problem common to most adaptive beamforming algorithms. Some popular solutions include directivity and derivative constraints [6]. These however would violate the spirit of blind separation since they require detailed prior knowledge of the signal. In the next subsection we show how the signal blocking matrix itself can be estimated blindly, thus greatly stabilizing the output gain.

D. Improved Hybrid GSC-like Implementation of Blind Algorithm Using Blindly Estimated Signal Blocking Matrix

The signal blocking matrix B can be estimated blindly using a canonical correlation-analysis-like scheme. Canonical correlation was first proposed by the statistician Hotelling in 1930s for determining dependencies between pairs of multivariate random vectors [7]. Suppose two random vectors have covariance matrix R_x and R_y respectively and cross-covariance matrix R_{xy}. Then the first canonical weights or coordinates are found by maximizing the cross-correlation

$$\max_{\vec{c}_{x1},\vec{c}_{y1}} \; \vec{c}_{x1}^{\,H} R_{xy} \vec{c}_{y1} \tag{9}$$

subject to $\mathrm{var}[\vec{c}_{x1}^{\,H}\vec{x}] = \mathrm{var}[\vec{c}_{y1}^{\,H}\vec{y}] = 1$. The remaining weights are found by successively solving

$$\max_{\vec{c}_{xk},\vec{c}_{yk}} \; \vec{c}_{xk}^{\,H} R_{xy} \vec{c}_{yk} \tag{10}$$

for k=2,...,M subject to the previous variance constraints and $\vec{c}_{xk}^{\,H} R_{xy} \vec{c}_{yj} = 0$, $\vec{c}_{xk}^{\,H} R_{xx} \vec{c}_{xj} = 0$, and $\vec{c}_{yk}^{\,H} R_{yy} \vec{c}_{yj} = 0$ for k≠j. The procedure for solving these equations is straightforward (modifying them to the complex-valued data case is easy) and can be found in most multivariate statistics texts (e.g.

see [7]). Since the nominal cross-covariance matrix is $R_{xy} = \sigma_s^2 \vec{s}\vec{s}^H$, the signal blocking matrix $B = [\vec{c}_2 \mid \vec{c}_3 \mid \cdots \mid \vec{c}_M]$ formed using the non-principal canonical weights must satisfy $B^H \vec{s} = 0$.

To estimate the signal blocking matrix B, the nominal quantities in (9) and (10) are replaced by their estimates and the principal canonical weight is set to the initial blind weight vector estimate, i.e., $\vec{c}_{x1} = \vec{c}_{y1} = \vec{w}'_{blind}$, and then are solved for the remaining weights. Our observation is that through empirical analysis, we have found that that the blind weight estimate provides a much superior estimate of the principal canonical weight than does the standard approach. The estimated signal blocking matrix is then plugged into GSC implementation depicted in fig. 4 and the blind filter weights are estimated again.

5 PSUEDO-SAS IMAGES

Finally pseudo-SAS acoustic intensity images (bearing vs. slant range only) were generated of the bottom using the data filtered by conventional beamforming (see fig. 6a) and the improved blindly estimated filter weights (see fig. 6b). We see that the blind method (fig. 6b) has significantly reduced snow-like interference and improved contrast compared to conventional beamforming in the regions labeled A, B, and C in fig. 6a.

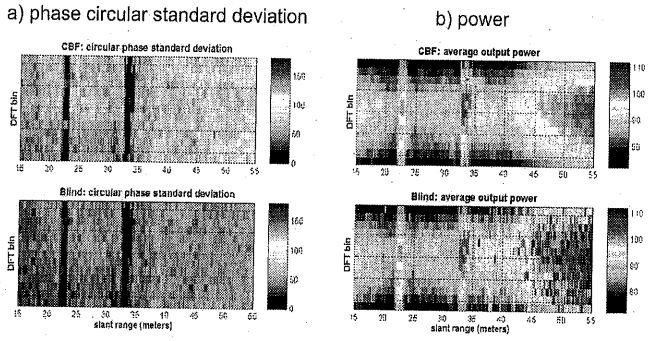

Figure 5. (a) The measured output ping-to-ping phase difference circular standard deviation (in degrees) plotted as function of DFT bin and slant range for the blind method (lower plot) and conventional beamformer (upper plot). (b) The measured mean output power (in decibels) plotted as function of DFT bin and slant range for the blind method (lower plot) and conventional beamformer (upper plot).

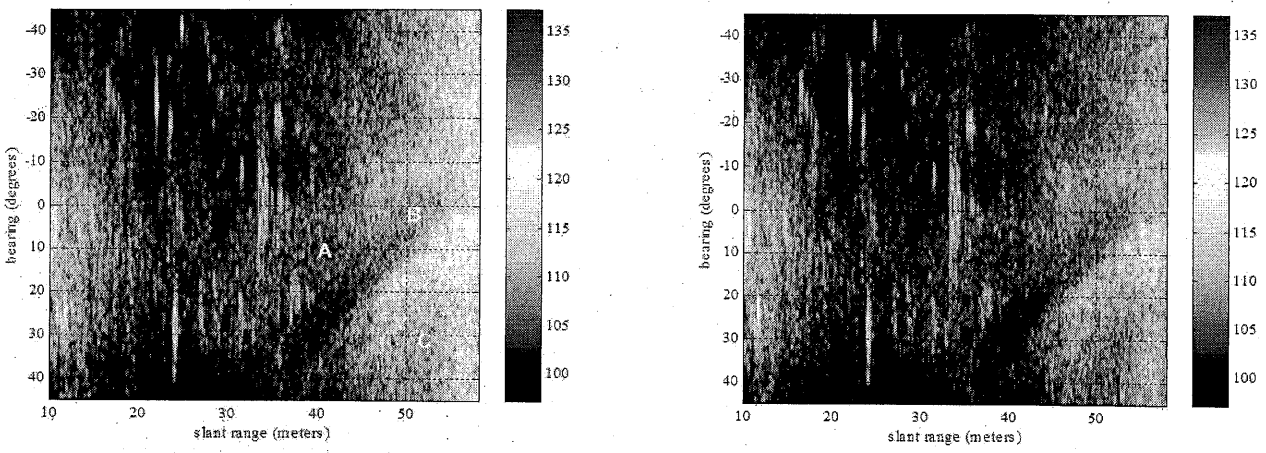

Figure 6. Pseudo-SAS image intensity in decibels for the (a) conventional beamformer and (b) blind separation method plotted as a function slant range vs. arrival angle.

6 LESSONS LEARNED AND CONCLUSION

Experimental implementation of array processing algorithms is non-trivial. The key challenge was not the estimation of the weight vector, but rather maintaining a constant signal response to enable accurate reconstruction of the time series from the spatially filtered frequency domain data. It was seen that relatively small errors in the assumed steering direction and array calibration can lead to large gain fluctuations that introduce errors and artifacts in the SAS image, even though from an output signal-to-noise ratio standpoint, the weight vectors were being estimated accurately.

The hybrid approach proposed here of using a GSC-like implementation of the blind method together with a blindly estimated signal blocking matrix is a viable way of maintaining a constant signal response without needing highly accurate array calibration and steering direction information. Although more work is needed, the new blind method works well in suppressing the multipath interference and is generally robust.

7 REFERENCES

1. J.E. Hudson, Adaptive Array Principles, Peter Peregrinus Ltd., 1981.
2. I.P. Kirsteins, "Blind Separation of Signal and Multipath Interference for Synthetic Aperture Sonar," in proc. of IEEE OCEANS-2003 conference, Sept. 2003.
3. A. Bellettini and M.A. Pinto, "Theoretical accuracy of synthetic aperture sonar micronavigation using a displaced phase center antenna," IEEE Journal of Oceanic Eng., vol. 27, no. 4, Oct. 2002, pp.780-789.
4. K.V. Mardia, Statistics of Directional Data, Academic Press 1972.
5. F. Asano et. al., "A combined approach of array processing and independent component analysis for blind separation of acoustic signals," IEEE Trans. on SP, vol. 11, no. 3, pp. 204-215, May 2003.
6. D.H. Johnson and D.E. Dudgeon, Array signal processing: Concepts and techniques, Prentice-Hall Signal Processing Series, 1993.
7. T.W. Anderson, An introduction to Multivariate Analysis: 2nd edition, John Wiley and Sons, 1984.